

# LHeC ERL DESIGN AND BEAM-DYNAMICS ISSUES

A. Bogacz, JLab, Newport News, VA 23606, USA

A. Latina, D. Schulte, CERN, Geneva, Switzerland

D. Pellegrini, EPFL, Lausanne, Switzerland and CERN, Geneva, Switzerland

## Abstract

The LHeC study is a possible upgrade of the LHC that aims at delivering an electron beam for collision with the existing hadronic beam. The current baseline design for the electron facility consists of a multi-pass superconductive energy-recovery linac operating in a continuous wave mode. Here, we describe the overall layout of such ERL complex located on the LHC site. We present an optimized multi-pass linac optics enabling operation of the proposed 3-pass RLA in the Energy Recovery mode. We also describe emittance preserving return arc optics architecture; including layout and optics of the arc switch-yard. High current (~100 mA) beam operation in the linacs excites long range wake-fields between bunches of different turns, which induce instabilities and might cause beam losses. The impact of long-range wake-fields, synchrotron radiation, and beam-beam effects has been assessed in this paper.

## INTRODUCTION

Two of the initially purposed options for the LHeC: the Linac-Ring and the Ring-Ring, both offered comparable performances. However, the Linac-Ring has recently been selected as the baseline; the choice mainly based on minimizing interference with the LHC operation. New sections of the lattice have been recently designed and a PLACET2 [1] simulation has been setup to validate the ERL operation.

The ERL based design for the LHeC electron facility is sketched in Fig. 1. Each of the two 1 km long superconducting linacs provide a total acceleration of 10 GeV. The injection energy is 500 MeV. In order to reach the collision energy of 60 GeV, the electrons are recirculated three times. Beams of different energies are directed into separate recirculation arcs via beam spreaders and recombiners placed at each end of the linacs. They allow to vertically separate the beams at the different energies routing them to the corresponding arcs. Arc2 and Arc4 are equipped with bypasses to avoid the interference with the detector.

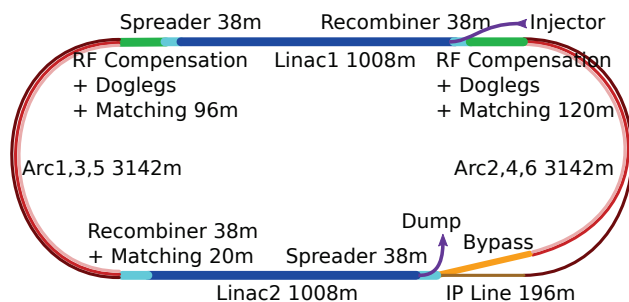


Figure 1: Scheme of the LHeC electron facility.

After the collision with the LHC proton or ion beam, the electron beam is decelerated in the subsequent three turns, allowing to increase the beam current and luminosity while limiting the power consumption [2]. The machine is operated continuously and bunches of different passes are interleaved in the linacs. An up-to-date beam parameter list can be found in [3].

## LATTICE COMPONENTS

### Linacs

The two linacs are about 1 km long and they consist of 18 FODO cells. Following each quadrupole two cryomodules are placed, each containing 8 cavities operating at 802 MHz, for a total of 576 cavities per linac. The phase advance per FODO cell is set to 130°. In order to reuse the same arcs for both the acceleration and deceleration, the  $\beta$  functions before and after each linac must coincide. The only free parameters are then the optic functions at the injection. These can be optimised minimising the value of:

$$\left\langle \frac{\beta}{E} \right\rangle = \int \frac{\beta}{E} ds$$

which enhances the impact of imperfections and many collective effects. Figure 2 shows the evolution of the Twiss functions in the linacs, starting from the initial condition.

### Arcs

To accomplish the multi-turn recirculation, six arcs are employed. They all share the same radius of 1 km. The lattice cell adopts a flexible momentum compaction layout which allows to tune each of them according to the impact of the Synchrotron Radiation at different energies. At the highest energy, it is crucial to minimise its emittance dilution tuning the cells to TME. At the lowest energy it is possible to compensate for the bunch elongation with a negative momentum compaction setup. The intermediate energy arcs are tuned to a DBA-like lattice, offering a good compromise. Fig. 3 shows the different tunings of the cells.

### Spreader and Recombiner

The spreaders and recombiners separate the bunches at different energies coming from the linac, in order to route them to the corresponding arc, and recombine them to the same orbit before entering the next linac.

The CDR design employs a two-step vertical bending that simplifies the suppression of the vertical dispersion. It has been verified that this design causes a non negligible energy loss, especially for Arc4, moreover it raises the horizontal  $\beta$  function to very high values. A new single-step design

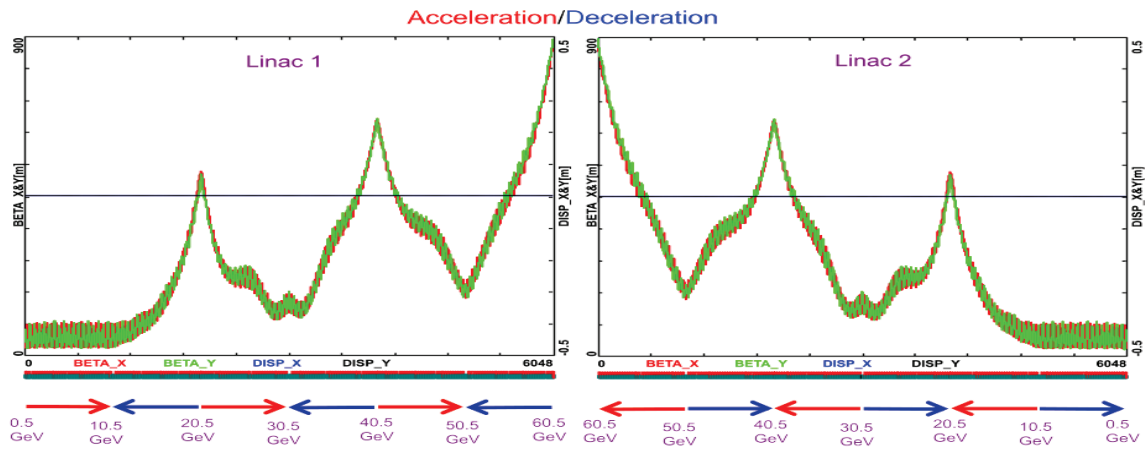


Figure 2: Optics functions in the linacs for the subsequent passages.

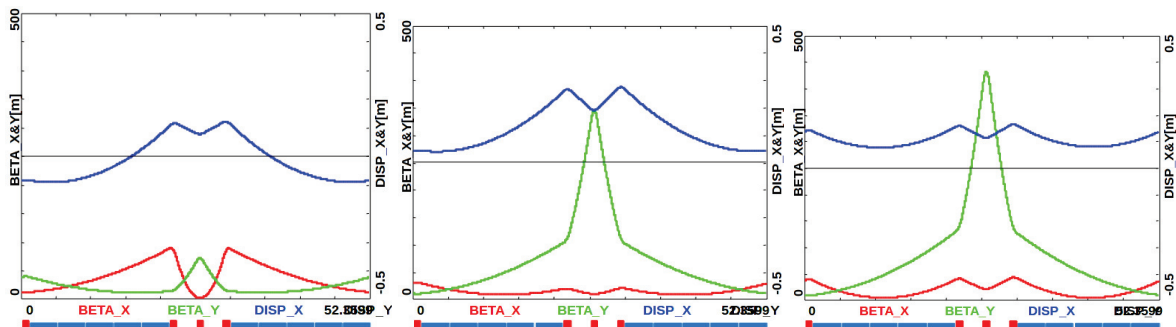


Figure 3: Cells for Arc1 and Arc2 (left), Arc3 and Arc4 (centre), Arc5 and Arc6 (right).

targets both. It employs seven quadrupoles to control the dispersion between the two bending dipoles. The energy loss is reduced by a factor 5 and at the same time both the dispersion and the  $\beta$  functions are reduced. The maximum quadrupole gradient of 80 T/m is not challenging adopting superconducting technology, but cannot be reached with warm magnets. The integrability of the systems needs to be verified with technical drawings. A comparison of the two design for the Arc2 spreader is shown in Fig. 4.

*Bypasses*

Following the spreader of linac2, that provides vertical separation, the 60 GeV beam goes straight to the IP; however, the lower energy beams need to be further separated to avoid the detector. This is accomplished by the bypass section that applies to Arc2 and Arc4. As shown in Fig. 1 and 5, the separation takes place in the horizontal plain, towards the inside of the racetrack. This allows one to minimise the required extra bending and therefore the impact of synchrotron radiation.

Ten arc-like dipoles, placed very close to the spreader, provide the initial bending, resulting in 10 m separation from the detector 150 m downstream. The straight section of the bypass is approximately 300 m long and may have many applications; such as diagnostic and path length adjustments. To connect with Arc6, ten of the sixty standard cells in Arc2

and Arc4, are replaced with seven higher field cells. This is a compromise between the field strength and length of the tunnel in which multiple-bore combined magnets [4] can be employed since the three arcs are vertically stacked.

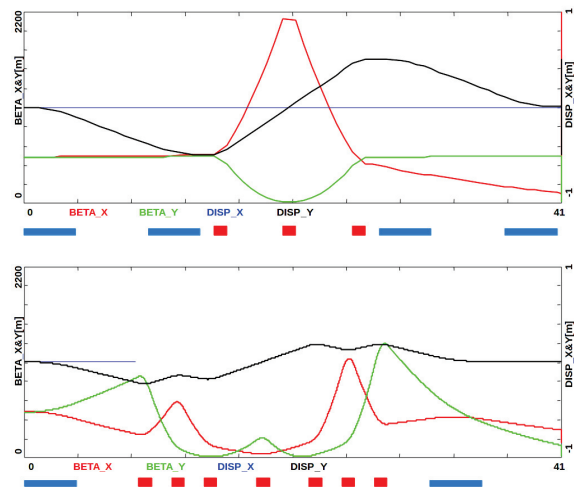


Figure 4: Optics functions for the two-steps vertical spreader (top) compared with the new design of a single-step spreader (bottom).

Figure 6 shows the Twiss functions at the beginning of Arc4. We chose to keep the same quadrupolar strengths in the junction and in the arc cells, this creates a little mismatch in the junction cells that is removed in the dispersion suppressor. In Arc2 the mismatch is more evident and it has been cured by adjusting the quadrupoles in the last junction cell and in the first regular cell.

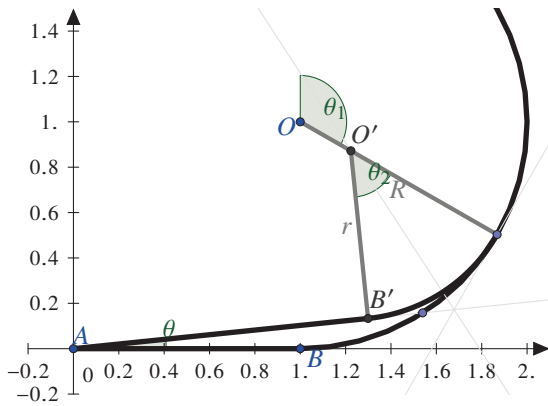


Figure 5: Scheme of the bypass geometry. The IP line,  $\overline{AB}$ , has been purposely stretched, being actually  $\sim 1/5$  of the arc radius.

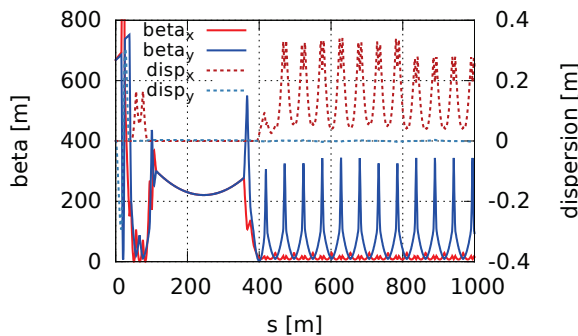


Figure 6: Beta functions and dispersion at the beginning of Arc4 with the detector bypass included. It features the vertical spreader, the initial horizontal bending, the straight section, the modified dispersion suppressor, seven junction cells, and four regular cells.

### Compensating RF

The energy lost due to the synchrotron radiation has to be replenished into the beam so that at the entrance of each arc the accelerating and decelerating beams have the same energy. Compensating cavities are placed before the bending section of Arc1, Arc3 and Arc5 and after the bending section of Arc2, Arc4 and Arc6. As shown in Fig. 7, they employ the second harmonic RF frequency, so that each section can replenish the energy lost in the corresponding arc for both the accelerating and the decelerating beams.

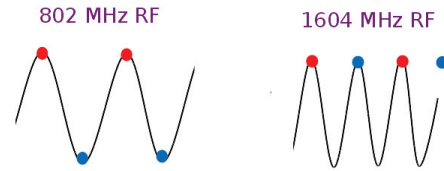


Figure 7: The second harmonic RF restores the energy loss both in the accelerating and decelerating passages.

## TRACKING SIMULATIONS

The two linacs and the six arcs, properly connected together, have been imported in PLACET2 [5]. This code implements the recirculation in a realistic way. Each element is defined only once and its phase is computed accordingly to the beam time of flight. The beam-beam effect is computed by GUINEA-PIG [6]. It has been found that the synchrotron radiation has a big impact in the spreader and recombiner sections and in the doglegs for path length adjustments. For the time being, in order to proceed with this study, the above effects have been ignored. The second harmonic RF, required to re-integrate the synchrotron radiation energy loss, is currently modelled as a thin element.

### Single-Bunch Tracking

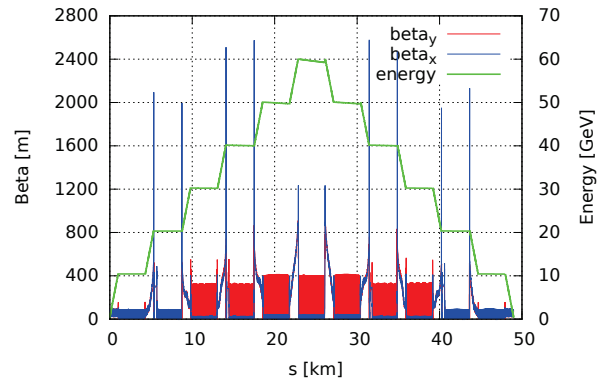


Figure 8: Beta functions and energy profile obtained following a bunch in the whole LHeC lattice.

The single bunch tracking allows to verify the beam transport. Figure 8 shows the Twiss parameters obtained following a bunch along its path along the whole machine. The linacs are easily identifiable by looking at the energy profile. In the arcs the energy stays almost constant, the only variation being caused by the synchrotron radiation. A small beta beating can be barely noted in the arcs: it is caused by the different model of the RF-focussing in the linacs between PLACET2 and OptiM, the program used for the matchings.

It is possible to note the different average values of the  $\beta$  functions in different arcs, deriving from their different tunings of the momentum compaction, as previously described.

The longitudinal phase space is shown in Fig. 9. It can be noted that while none of the arc is isochronous, their combined effects preserve the bunch length reducing the impact

of the RF curvature. The beam parameters are summarised in Table 1 and Table 2 respectively at the IP and at the dump (after the deceleration). The beam is transported to the IP with a reasonable emittance growth. The impacts of beam-beam and SR in Arc6 are evident, but not detrimental to the deceleration. The beam envelop remains well within the aperture even at the end of the deceleration as shown in Fig. 10.

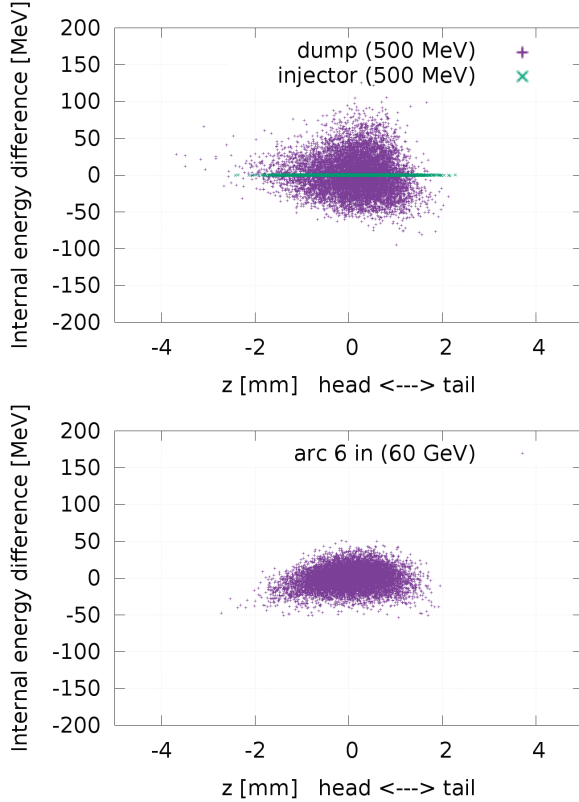


Figure 9: Longitudinal phase space at the injection and dump (top) and at the IP (bottom). The zero of the vertical axis is the value indicated in the key.

Table 1: Initial Beam Parameters Compared To The Ones At The IP In Presence Of Synchrotron Radiation

	initial/CDR	IP
$\varepsilon_x$ [ $\mu\text{m}$ ]	50	57.4
$\varepsilon_y$ [ $\mu\text{m}$ ]	50	50.8
$\delta$	0.0020	0.0026
RMS x [ $\mu\text{m}$ ]	7.20	7.66
RMS y [ $\mu\text{m}$ ]	7.20	7.21
RMS z [mm]	0.600	0.601
RMS e [MeV]	1.00	15.4

### Multi-Bunch Effects

PLACET2 allows to set up a train of bunches for tracking. It simultaneously propagates all the bunches in the machine preserving their time sequence in each beamline. This allows to compute multi-bunch effects even with complex lattice

topologies. A model of transverse long-range wakefields (LRW) is currently implemented in PLACET2. LRW take place when a bunch passing through a cavity excites higher order modes (HOMs) of oscillation of the electromagnetic field; if the Q-value is big enough, the HOMs kick the subsequent bunches. High current and strong HOMs can establish a positive feedback leading to beam break up. The operation of the LHeC as an Higgs Factory requires high currents, up to 150 mA in the linacs [3], this posed a concern for the beam stability.

Table 2: Beam Parameters At The Dump, The Columns Shows The Values For SR Only, SR And Beam-Beam, SR And Beam-Beam With High-Lumi Parameters. The List Of Parameters Can Be Found In [3].

	Final SR	SR + BB	SR + BB-HL
$\varepsilon_x$ [ $\mu\text{m}$ ]	107	133	165
$\varepsilon_y$ [ $\mu\text{m}$ ]	87	125	158
$\delta$	0.059	0.059	0.059
RMS x [mm]	1.52	1.67	1.86
RMS x' [mrad]	0.08	0.09	0.10
RMS y [mm]	2.42	3.03	3.15
RMS y' [mrad]	0.07	0.09	0.09
RMS z [mm]	0.66	0.66	0.66
RMS e [MeV]	29.7	29.5	29.6

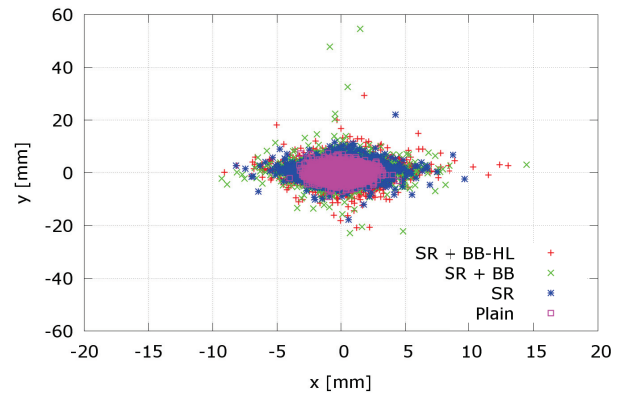


Figure 10: Beam transverse section at the end of the last linac, after the deceleration, including Synchrotron Radiation and Beam-Beam with standard and High Luminosity parameters. The beam contains 5000 macroparticles and the initial distribution is gaussian with no cuts.

For the multi-bunch simulation the same setup, as described before, was used. The tracking was performed using single particle bunches. The beam-beam computation GUINEA-PIG was substituted by an amplitude-dependent kick. The simplified beam-beam calculation overestimates the beam-beam effect as in reality the electrons oscillate around the proton beam and receive a smaller kick. The HOMs considered are the transverse dipole modes of the SPL cavity design, scaled to 802 MHz.

In order to evaluate the LRW impact the machine is completely filled with approximately 6000 single-particle

bunches perfectly aligned. One misaligned bunch is then injected followed by many bunches again perfectly aligned. The perturbation introduced by the misaligned bunch is propagated to the others, as can be seen in Fig. 11. There are two important parameters: the slope of the tail, which determines if and how fast the perturbation is damped; and the  $F$  parameter that represents the total amplification of the beam action, defined as the squared sum of all the amplitudes [7]. This sum is convergent and mostly driven by the bunches that are close to the exciting one.

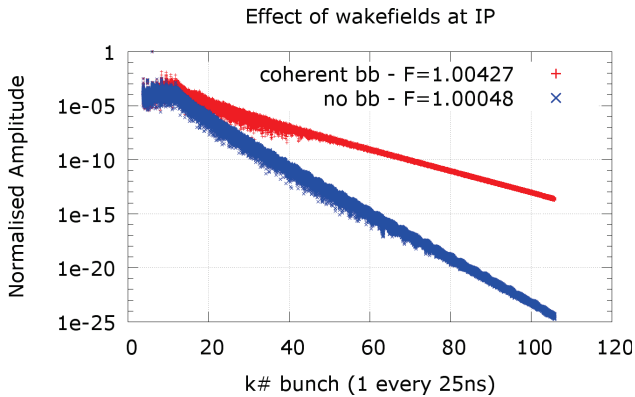


Figure 11: Normalised actions of the bunches at the IP. Only the bunch with action 1 carries an initial misalignment. All the other bunches are excited by LRW. Each bunch contains  $4 \times 10^9$  electrons.

### BUNCH RECOMBINATION PATTERN

The LHeC operation foresees continuous injection and multi-turn recirculation. In this scenario more bunches at different energies are interleaved in the linacs, appearing in periodic sequences. The spreader and recombiner design, employing fixed-field dipoles, do not pose timing constraints. This gives us full control of the recombination pattern that can be selected adjusting the length of the return arcs to the required integer number of  $\lambda$ .

A good choice for the recombination pattern consists of almost equal spacing (compatibly with the RF) of the bunches in the RF buckets. In order to minimise the bunch cross talk it is advantageous to maximise the separation between the bunches at the lowest energy: the ones at first and sixth turn. This is depicted in Fig. 12.

It has been verified that a pattern where bunches at first and sixth turn closely follow each other, reduces the BBU threshold current.

### CONCLUSIONS AND OUTLOOK

The LHeC study is vigorously progressing both on the lattice design and on the beam dynamics simulations. In this paper we have reviewed the fundamental components of the LHeC lattice together with their optimisations. The machine layout, the linacs and the return arcs design have been summarised and new sections such as the detector bypass and the single-step spreader have been introduced.

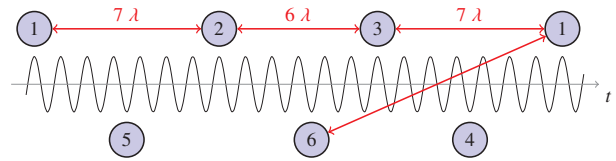


Figure 12: When the recirculation is in place, the linacs are populated with bunches at different turns (the turn number is indicated).

A comprehensive simulation has been setup using the newly developed tracking code: PLACET2. The impacts of synchrotron radiation, long-range wakefields and beam-beam effect have been evaluated and they are not detrimental for the deceleration. Investigation of cavity misalignment impact on beam trajectories has also been initiated.

The next major steps should target the full integration of the lattice with the interaction region. Realistic simulation of the ion cloud effect should also be performed. Furthermore detailed estimate of tolerances in terms of field quality and phase stability are required and may come with the experimental support of the CERN ERLF [8], currently in the design phase.

### ACKNOWLEDGMENT

The authors would like to thank Edward Niessen for his help with the GUINEA-PIG computations of the beam-beam effect.

### REFERENCES

- [1] D. Pellegrini et al., “PLACET2: a Novel Code for Beam Dynamics in Recirculating Machines”, MOPJE068, Proceedings of IPAC’15, Richmond VA, USA (2015).
- [2] J.L. Abelleira Fernandez et al., “LHeC Conceptual Design Report”, J. Phys. G: Nucl. Part. Phys. 39 075001 (2012).
- [3] F. Zimmerman, O. Brüening, M. Klein, “The LHeC as a Higgs Boson Factory”, MOPWO054, IPAC’13, Shanghai, China (2013).
- [4] A. Milanese, “Warm magnets for LHeC / Test Facility arcs”, Talk at the LHeC workshop 2014, <https://indico.cern.ch/event/278903/session/6/contribution/41>
- [5] D. Pellegrini et al., “Single and Multi-bunch End-to-end Tracking in the LHeC”, MOPJE066, Proceedings of IPAC’15, Richmond VA, USA (2015).
- [6] D. Schulte, “Beam-Beam Simulations with GUINEA-PIG”, ICAP’98, Monterey CA, USA (1998).
- [7] D. Schulte, “Multi-Bunch Calculations in the CLIC Main Linac”, FR5RFP055, Proceedings of PAC09, Vancouver, BC, Canada.
- [8] E. Jensen et al., “Design Study of an ERL Test Facility at CERN” TUOBA02, Proceedings of IPAC’14, Dresden, Germany (2014).